euronoise

Stochastic modeling of the vibro-acoustic behavior of production cars

Laurent Gagliardini[a], Jean-Francois Durand[b] and Christian Soize[c]

[a]PSA Peugeot Citroën, Route de Gisy, 78943 Vélizy-Villacoublay Cedex, France
[b]Université Paris-Est, Laboratoire de Mécanique, 5 bd Descartes, 77454 Marne-la-Vallée, France
[c]Université de Marne la Vallée, 5, Boulevard Descartes, 77454 Marne la Vallée, France
laurent.gagliardini@mpsa.com

Production cars -as any industrial product- are subjecteded to various causes of variability including process uncertainties or product diversity. Many authors have shown that vibroacoustic problems sensitivity to small uncertainties increases dramatically with frequency and that only statistical approaches remain relevant in the high-frequency range. Moreover, modeling uncertainties due to numerous model simplifications induce similar dispersion effects on the computed responses. Both kind of uncertainties may be addressed when using a nonparametric stochastic modeling, based on the random matrix theory. Such a modeling appears to be very practicable for industrial vibroacoustic problems while relying on a strong mathematical background. In a first part, the application of the non-parametric modeling of uncertainties to vibroacoustic problems will be addressed. Stochastic aspects are controled by only 7 dispersion parameters that provide most of the dynamic behaviors that can experimentally be observed. A Monte-Carlo simulation is performed to provide converged statistics of the stochastic problem solution. In a second part, the dispersion parameters are identified so that the stochastic model fits experimental data. Frequency Response Functions of 20 production vehicles were measured for this purpose and compared to the computed results in the low frequency range (<200 Hz).

1 Introduction

The NVH design of cars is nowadays mainly based on computational models that provide structural vibrations and internal acoustic levels simulations to be optimized toward customer needs and production costs.

Considering the very high complexity of such a structural-acoustic system, as well as the so-called dynamic hypersensitivity, some modeling errors - induced for instance by engineering simplifications - lead to significant prediction errors. The other way round, production cars, including their diversity and variability, exhibit a significant amount of dispersion. In order to improve the robustness of the computational structural-acoustic model regarding production reality, both model and data uncertainties have to be taken into account. In this context, a non-parametric probabilistic approach of uncertainties is implemented in a conventional computational structural-acoustic model.

The aim of this paper is the assessment of the proposed stochastic modeling for automotive applications and the identification of the parameters controlling the amount of uncertainty. Relevant experiments have been developed on purpose, in order to constitute a significant experimental database including structural vibrations and internal cavity acoustic pressures. This database will later be used to proceed to the experimental identification of the parameters and to validate the computational model.

Experimental results are presented first in order to focus on the application case. Then, the non-parametric stochastic modeling of vibroacoustic problems will be shortly addressed. Once the control parameters of the stochastic model are defined, they have to be identified to specific observations of real cars. At last, the stochastic prediction of a partial estimation of the booming noise - using optimized dispersion parameters- is compared to measured values.

This paper is mainly based on [1,2].

2 Production vehicles dispersion measurement

Experiments which are described here were performed in PSA Peugeot-Citroën facilities. The system under consideration is the full vehicle for which two sets of experiments have been defined. The first set is made up of measurements of the structural vibration and structural-acoustic responses. The second set is devoted to the acoustic measurements inside the internal acoustic cavity.

2.1 Structural and vibroacoustic measurements

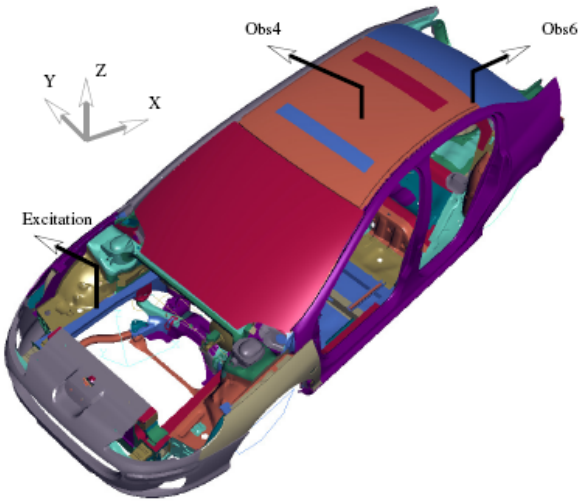

Fig.1 Car body, structural excitation and observation

The first set of experiments consists, (i), in measuring structural Frequency Response Functions (FRFs) between a force (vertical component of the powertrain right mount action) and normal accelerations of the structure at six given points and, (ii), in measuring structural-acoustic FRFs between nine excitation Degrees Of Freedom (DOFs) at the powertrain connection point and the acoustic pressure at the driver ears. The frequency band of analysis is [20, 220] Hz. The experimental database has been constructed using 20 cars of the same type with various optional extras. Measurements have been performed at the exit of the assembly plant. Fig.1 shows the car body, the structural driving point (vertical excitation) and two structural observation points (denoted by Obs4 and Obs6). In this paper, experimental results will only be presented for point Obs6.

Fig.2 displays the experimental structural FRFs introduced above for observation point Obs6 and for the 20 measured cars. This experimentally observed dispersion is mainly due to the variability of the samples induced by the optional

extras and by the manufacturing process. Measurements errors as well as atmospheric conditions may also contribute to the spread of results. This observed dispersion is increasing with the frequency, in coherence with published results [3]. The experimental dispersion varies between 5 and 10 dB in the regions close to the resonances, and varies from 15 to 30 dB close to anti-resonances.

Vibroacoustic FRF's will not be presented individually. They will be synthesized in an estimate of the booming noise (2^{nd} engine harmonic vs rpm), obtained by multiplying each of the FRF by an associated known force, and adding up all contributions. Such estimate of the booming noise may be seen in the background of Fig. 8.

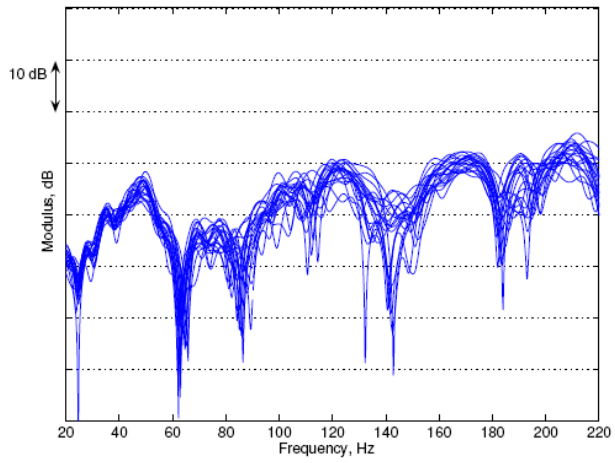

Fig.2 Structural FRF modulus at point Obs6 for the 20 measured cars

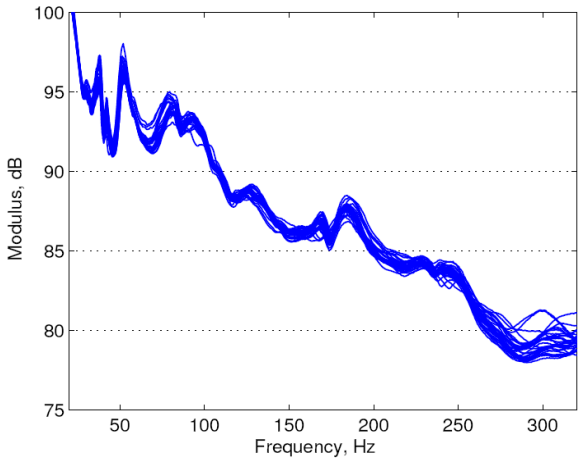

Fig.3 Car compartment energy of 20 measurements with environmental and packaging changes

2.2 Acoustic measurements

The second set of experiments consists in measuring the acoustic FRFs between the acoustic pressures at 32 points inside the internal acoustic cavity and an acoustic velocity point-source located near the feet of the front passenger. In order to synthesize results, the energy of the cavity is computed:

$$E(f) = \frac{V}{\rho c^2}\frac{1}{32}\sum_1^{32} p_i^2(f)$$

This experimental database has been constructed for 30 different configurations of internal acoustic cavity of a same car: type and position of seats, air temperature, wall boundaries between the trunk and the passenger compartment, number of passengers. The frequency band of analysis is [20, 320] Hz. Fig. 3 displays the 30 spectra of the cavity energy that were measured. It can be noticed that the order of magnitude of dispersion is much lower than in the previous case (Fig.2): indeed, energy is known as a robust state variable.

3 Nonparametric stochastic modeling of a structural-acoustic problem

The structural-acoustic coupling problem, such as the one existing in a car, is expressed as a general boundary value problem, as explained in [4]. Most kind of boundary conditions as well as mechanical behavior for the structure and the cavity are supported. Fig. 4 shows the scheme of the considered idealized system including a structural part, surrounding an acoustic cavity.

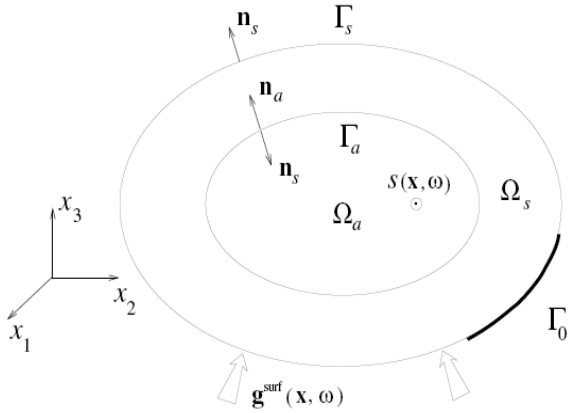

Fig.4 Scheme of the idealized structural-acoustic system

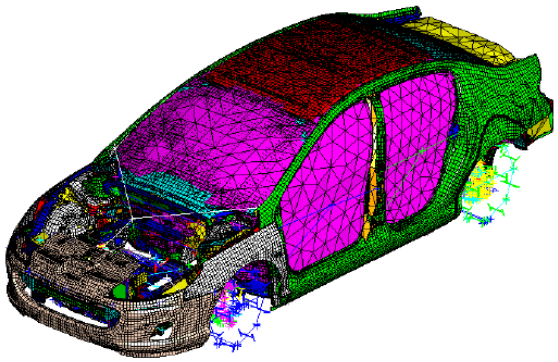

Fig.5 Finite Elements mesh of the computational structural-acoustic model (978 733 DOF's)

3.1 Mean computational model

The finite element method [5] is used to solve numerically the above mentioned boundary value problem in a

deterministic case. The resulting FE model will later be referred as "mean computational model". Let us consider the finite element meshes of the structure and the internal acoustic fluid as shown on Fig.5. Such FE models are obtained following specific modeling rules [6].

Let $\underline{\mathbf{u}}^{s}$ (resp. $\underline{\mathbf{p}}^{a}$) be the complex vector of the n_s (resp. n_a) DOFs of the structure (resp. acoustic cavity) according to the finite element discretization of the displacement field u (resp. pressure field p). The finite element discretization of the boundary value problem in terms of u and p yields the mean computational structural-acoustic model:

$$\begin{bmatrix} \underline{\mathbf{A}}^{s}_{\mathbf{n}_s}(\omega) & \underline{\mathbf{C}}_{\mathbf{n}_s,\mathbf{n}_a} \\ \omega^2 \underline{\mathbf{C}}_{\mathbf{n}_s,\mathbf{n}_a}{}^{\mathrm{T}} & \underline{\mathbf{A}}^{a}_{\mathbf{n}_a}(\omega) \end{bmatrix} \begin{bmatrix} \underline{\mathbf{u}}^{s}(\omega) \\ \underline{\mathbf{p}}^{a}(\omega) \end{bmatrix} = \begin{bmatrix} \underline{\mathbf{f}}^{s}(\omega) \\ \underline{\mathbf{Q}}^{a}(\omega) \end{bmatrix}$$

$\underline{\mathbf{A}}^{s}_{\mathbf{n}_s}(\omega)$ is the dynamic stiffness matrix of the damped structure, such that $\underline{\mathbf{A}}^{s}_{\mathbf{n}_s}(\omega) = -\omega^2 \underline{\mathbf{M}}^{s}_{\mathbf{n}_s} + j\omega \underline{\mathbf{D}}^{s}_{\mathbf{n}_s} + \underline{\mathbf{K}}^{s}_{\mathbf{n}_s}$ where $\underline{\mathbf{M}}^{s}_{\mathbf{n}_s}, \underline{\mathbf{D}}^{s}_{\mathbf{n}_s}, \underline{\mathbf{K}}^{s}_{\mathbf{n}_s}$ are respectively the mass, damping and stiffness matrices of the studied structure.

$\underline{\mathbf{A}}^{a}_{\mathbf{n}_a}(\omega)$ is the admittance matrix of the damped blocked cavity, such that $\underline{\mathbf{A}}^{a}_{\mathbf{n}_a}(\omega) = -\omega^2 \underline{\mathbf{M}}^{a}_{\mathbf{n}_a} + j\omega \underline{\mathbf{D}}^{a}_{\mathbf{n}_a} + \underline{\mathbf{K}}^{a}_{\mathbf{n}_a}$ where $\underline{\mathbf{M}}^{a}_{\mathbf{n}_a}, \underline{\mathbf{D}}^{a}_{\mathbf{n}_a}, \underline{\mathbf{K}}^{a}_{\mathbf{n}_a}$ are -abusively- named the mass, damping and stiffness matrices of the cavity.

$\underline{\mathbf{C}}_{\mathbf{n}_s,\mathbf{n}_a}$ is the vibroacoustic coupling matrix.

It is a common practice to proceed to a model reduction by mean of a projection over the eigenvectors -modes- of the undamped problems for the structure and for the cavity. In the application shown on Fig.5, 1723 structural modes and 57 acoustic modes were considered.

For the structure and the cavity, the generalized coordinates, $\underline{\mathbf{q}}_{\Psi}{}^{s}(\omega), \underline{\mathbf{q}}_{\Phi}{}^{a}(\omega)$, are introduced such as:

$$\underline{\mathbf{u}}^{s}(\omega) = \underline{\boldsymbol{\Psi}} \underline{\mathbf{q}}_{\Psi}{}^{s}(\omega)$$
$$\underline{\mathbf{p}}^{a}(\omega) = \underline{\boldsymbol{\Phi}} \underline{\mathbf{q}}_{\Phi}{}^{a}(\omega)$$

The structural-acoustic problem can then be set in the reduced form:

$$\begin{bmatrix} \underline{\mathbf{A}}^{s}_{\Psi}(\omega) & \underline{\mathbf{C}}_{\Psi,\Phi} \\ \omega^2 \underline{\mathbf{C}}_{\Psi,\Phi}{}^{\mathrm{T}} & \underline{\mathbf{A}}^{a}_{\Phi}(\omega) \end{bmatrix} \begin{bmatrix} \underline{\mathbf{q}}_{\Psi}{}^{s}(\omega) \\ \underline{\mathbf{q}}_{\Phi}{}^{a}(\omega) \end{bmatrix} = \begin{bmatrix} \underline{\mathbf{f}}_{\Psi}{}^{s}(\omega) \\ \underline{\mathbf{Q}}_{\Phi}{}^{a}(\omega) \end{bmatrix}$$

where the reduced dynamic stiffness matrix, $\underline{\mathbf{A}}^{s}_{\Psi}(\omega)$, and the reduced admittance matrix, $\underline{\mathbf{A}}^{a}_{\Phi}(\omega)$, have similar expression as above:

$$\underline{\mathbf{A}}^{s}_{\Psi}(\omega) = -\omega^2 \underline{\mathbf{M}}^{s}_{\Psi} + j\omega \underline{\mathbf{D}}^{s}_{\Psi} + \underline{\mathbf{K}}^{s}_{\Psi}$$
$$\underline{\mathbf{A}}^{a}_{\Phi}(\omega) = -\omega^2 \underline{\mathbf{M}}^{a}_{\Phi} + j\omega \underline{\mathbf{D}}^{a}_{\Phi} + \underline{\mathbf{K}}^{a}_{\Phi}$$

In this case, mass and stiffness matrices are diagonal, thanks to the orthogonality property. Reduced damping matrices are generally full symmetric matrices.

3.2 Nonparametric stochastic modeling

As stated in introduction, both data and model uncertainties have to be accounted in order to improve the robustness of simulations for cars in mass production. The nonparametric probabilistic approach is a well defined mathematical method [7,8], providing a stochastic modeling of any physically possible changes of the mean computational model . It consists in modeling the reduced mass, damping and stiffness matrices of both structure and cavity, as well as the reduced vibroacoustic coupling matrix,

$$\underline{\mathbf{M}}^{s}_{\Psi}, \underline{\mathbf{D}}^{s}_{\Psi}, \underline{\mathbf{K}}^{s}_{\Psi}, \underline{\mathbf{M}}^{a}_{\Phi}, \underline{\mathbf{D}}^{a}_{\Phi}, \underline{\mathbf{K}}^{a}_{\Phi}, \underline{\mathbf{C}}_{\Psi,\Phi}$$

by random matrices:

$$\mathbf{M}^{s}_{\Psi}, \mathbf{D}^{s}_{\Psi}, \mathbf{K}^{s}_{\Psi}, \mathbf{M}^{a}_{\Phi}, \mathbf{D}^{a}_{\Phi}, \mathbf{K}^{a}_{\Phi}, \mathbf{C}_{\Psi,\Phi}$$

Let $\mathbf{H}$ be anyone of these random matrices. The probability density function of such a random matrix $\mathbf{H}$ only depends on:

- the mean value $\underline{\mathbf{H}} = E\{\mathbf{H}\}$ where E is the mathematical expectation,
- one single dispersion parameter , $\delta_{\mathbf{H}}$, which is independent of the matrix dimension.

An algebraic representation of random matrix $\mathbf{H}$ has been developed and allows independent realizations to be constructed for a stochastic solver based on the Monte Carlo numerical simulation. For random matrices $\mathbf{M}^{s}_{\Psi}, \mathbf{D}^{s}_{\Psi}, \mathbf{K}^{s}_{\Psi}, \mathbf{M}^{a}_{\Phi}, \mathbf{D}^{a}_{\Phi}, \mathbf{K}^{a}_{\Phi}$, random matrix $\mathbf{H}$ is a symmetric positive-definite (or positive-semidefinite) real-valued random matrix which may be written as

$$\mathbf{H} = \mathbf{L}_{\mathbf{H}}{}^{t} \mathbf{G}_{\delta_{\mathbf{H}}} \mathbf{L}_{\mathbf{H}}$$

where $\mathbf{G}_{\delta_{\mathbf{H}}}$ is a random germ matrix whose mathematical expectation is the identity matrix and for which the square of the coefficient of variation is $\delta_{\mathbf{H}}{}^{2}$.

The case of the rectangular random vibroacoustic coupling matrix, $\mathbf{C}_{\Psi,\Phi}$, will not be treated in this paper and we refer the reader to [1,2].

The stochastic reduced model of the uncertain structural-acoustic system is expressed, for all ω fixed in the frequency band of analysis, as:

$$\begin{bmatrix} \mathbf{A}^{s}_{\Psi}(\omega) & \mathbf{C}_{\Psi,\Phi} \\ \omega^2 \mathbf{C}_{\Psi,\Phi}{}^{\mathrm{T}} & \mathbf{A}^{a}_{\Phi}(\omega) \end{bmatrix} \begin{bmatrix} \mathbf{q}_{\Psi}{}^{s}(\omega) \\ \mathbf{q}_{\Phi}{}^{a}(\omega) \end{bmatrix} = \begin{bmatrix} \underline{\mathbf{f}}_{\Psi}{}^{s}(\omega) \\ \underline{\mathbf{Q}}_{\Phi}{}^{a}(\omega) \end{bmatrix}$$

The observed random responses of the uncertain structural-acoustic problem are the random structural displacements and the random acoustic pressures, deduced from the random generalized coordinates:

$$\mathbf{u}^{s}(\omega) = \underline{\boldsymbol{\Psi}} \mathbf{q}_{\Psi}{}^{s}(\omega)$$
$$\mathbf{p}^{a}(\omega) = \underline{\boldsymbol{\Phi}} \mathbf{q}_{\Phi}{}^{a}(\omega)$$

The solutions obtained for successive independent realizations of this random vibroacoustic system are constructed using the Monte-Carlo method which allows statistics of the random observations to be estimated. The confidence regions associated with a given probability level are obtained using the method of quantiles [9]. In the following, stochastic computation results will be

represented by their mean value and their confidence interval with a probability level of 95%. It was verified that the Monte-Carlo method requires about 600 realizations to reach convergence.

4 Dispersion parameters identification

Once the stochastic model of the studied vibroacoustic system is set up, then its application requires the knowledge of the dispersion parameters associated with the 7 matrices involved in the structural-acoustic system. Two different methodologies are applied one for the cavity and the other one for the structure.

4.1 Acoustic dispersion parameters

Dispersion parameters $\delta_{\mathbf{M_a}}, \delta_{\mathbf{K_a}}, \delta_{\mathbf{D_a}}$ of the internal acoustic cavity are identified using the experimental database defined in Section 2.2. For this identification, it is assumed that $\delta_{\mathbf{M_a}} = \delta_{\mathbf{K_a}} = \delta_{\mathbf{D_a}} = \delta_a$. Various analyses have shown that the sensitivity of confidence regions to acoustic mass and stiffness dispersion parameters were similar. Moreover, confidence regions appeared to be not very sensitive to the damping dispersion parameter. In this context, the above assumption allows the computational cost to be drastically decreased when considering only one variable instead of three.

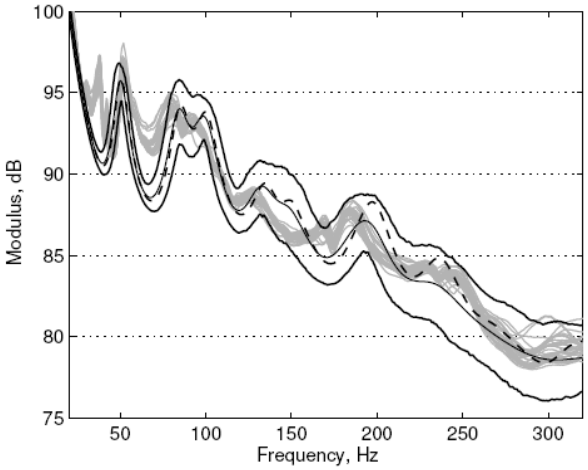

Fig.6 Comparison of the stochastic modeling of the cavity energy (solid black lines: average value and 95% confidence interval) with experimental results (grey solid lines) and mean computational model (dotted black line).

The identification method used to identify the acoustic dispersion parameter is the maximum likelihood method [10,11]. The likelihood function is defined as the product of the probability density functions evaluated at each experimental data. In practice, the log-likelihood function is used:

$$\angle(\delta_a) = \sum_i \log_{10}\left(p_Y\left(\delta_a, Y_i^{\exp}\right)\right)$$

where $p_Y(\delta_a, y)$ is the probability density function of the random observation Y computed with the stochastic model for a given value of the dispersion parameter δ_a.

The identification problem can then be formulated as the following optimization problem:

$$\delta_a^{opt} = \underset{\delta_a}{Arg\,\max}\{\angle(\delta_a)\}$$

It should be noted that this methodology requires an estimate of the probability density function which requires a large number of independent realizations in the Monte-Carlo method.

For this application, the random observation Y is defined by

$$Y_i = \int_{[20-320]} 10\log_{10}(E_i(f))df$$

Fig. 6 compares the result of the optimized model with the experiments. Although the trend seems to be good, the model often overestimates the upper limit of the experimental spread. This is due to the necessary introduction of model uncertainties whose intensity is measured by the value of the dispersion parameter.

4.2 Structural dispersion parameters

Structural dispersion parameters are identified from the structural measurements described in Section 2.1. In this case, the assumption that the 3 dispersion parameters are equal can not be made anymore. Mass and stiffness dispersion parameters lead to different effects (see [1]).

Due to the size of the computational model and due to the fact that three parameters have to be identified, a more conventional "mean-square" methodology, less time consuming, is chosen. The identification of the dispersion parameters is written as the following optimization problem:

$$\boldsymbol{\delta}_s^{opt} = \underset{\boldsymbol{\delta}_s}{Arg\,\min}\{J(\delta_s)\}$$

where $J(\delta_s)$ is an error function that is the sum of two norms. The first norm represents the variance of the computational model due to uncertainties and the second norm represents the bias between the experiments and the stochastic model:

$$J(\delta_s) = \left\|\left\|Z(\delta_s) - \underline{Z}(\delta_s)\right\|\right\|^2 + \left\|\underline{Z}^{\exp} - \underline{Z}(\delta_s)\right\|^2$$

with

$$\left\|\left\|Z(\delta_s) - \underline{Z}(\delta_s)\right\|\right\|^2 = E\left\{\sum_j \int_B \left|Z_j(\omega,\delta_s) - \underline{Z}(\omega,\delta_s)\right|^2 d\omega\right\}$$

$$\left\|\underline{Z}^{\exp} - \underline{Z}(\delta_s)\right\|^2 = \sum_j \int_B \left|\underline{Z}_j^{\exp}(\omega) - \underline{Z}(\omega,\delta_s)\right|^2 d\omega$$

where Z represents any relevant random observation.

For this first application, the optimization was performed using a response surface.

Once the optimal values of the dispersion parameters are obtained, results of the optimal reduced stochastic model can be compared with the experimental results. Fig.7 compares the structural FRF between the right engine mount and point Obs4. As it was the case for the acoustic cavity, the general trends are well respected. Again the confidence interval of the computational model is much higher than the experimental spread. This is due to the amount of dispersion that was required to compensate

model uncertainties or modeling errors which effects clearly appear on Fig.7.

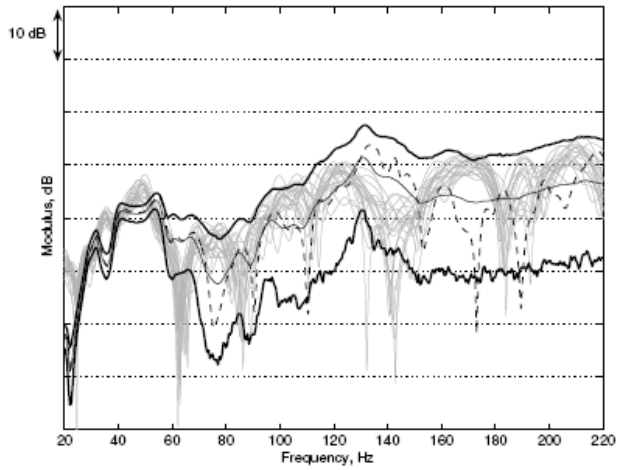

Fig.7 Structural FRFs at point Obs6: Comparison of the stochastic modeling (solid black lines: average value and 95% confidence interval) with experiments (grey solid lines) and mean computational model (dotted black line).

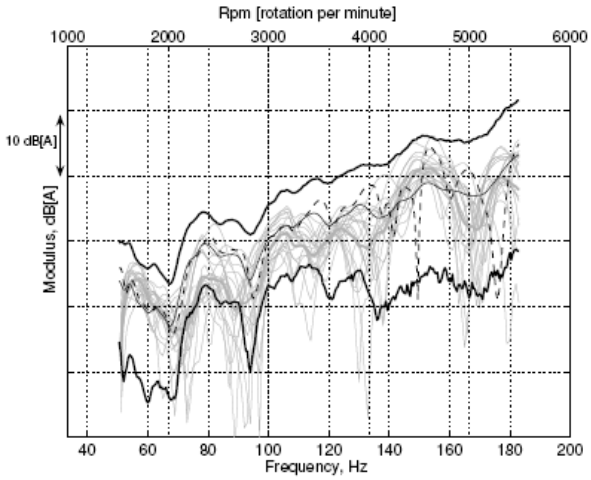

Fig.8 Booming noise estimate: Stochastic computation using the optimized dispersion parameters modeling (solid black lines: average value and 95% confidence interval) compared with experimental values (grey solid lines) and mean computational model (dotted black line).

5 Experimental validation of the stochastic computational structural-acoustic model for the booming noise

Since direct measurements were not available, an estimate of the booming noise is built from the vibroacoustic FRFs as explained in section 2.1. The same forces may be applied to the model to get simulated values of the same estimate of the booming noise. This approach allows focusing on the car body uncertainties apart from engine excitations uncertainties. Figure 8 shows a comparison of the stochastic computational model results with experimental results. General trends are very similar and the agreement seems even better than what was observed in Fig.6 and 7.

6 Conclusions

A stochastic modeling of the structural-acoustic problem, including data and model uncertainties, have been presented and applied to the low-frequency noise in a car. Dispersion parameters of this first model have been fitted to an experiment involving 20 production vehicles. Two different identification methods have been investigated providing satisfactory results. Due to model uncertainties, the predicted confidence interval remains much larger than the spread of experimental results. Nevertheless, experimental results are mostly covered by the confidence interval of the stochastic prediction, which assess the relevance of this kind of stochastic modeling for automobile applications.

References

[1] Durand, J.F."Structural-acoustic modeling of automotive vehicles in presence of uncertainties and experimental identification and validation," PHD Thesis, Université de Marne-la-Vallée, France, (2007)

[2] Durand J.-F., Soize C., Gagliardini L. "Structural-acoustic modeling of automotive vehicles in presence of uncertainties and experimental identification and validation" *accepted for publication in JASA (2008)*

[3] Hills, E., Mace, B., and Ferguson, N.S "Statistics of complex built-up structures," *International Conference on Modal Analysis Noise and Vibration Engineering (ISMA 2004) proceedings* CDROM ISBN 90-73802-82-2 (2004)

[4] Ohayon, R., and Soize, C." Structural Acoustics and Vibration", Academic Press, San Diego. (1998)

[5] Zienkiewicz, O. C., and Taylor, R. L."The Finite Element Method", Fifth edition,Vol. 1 to 3, Butterworth-Heinemann, Oxford, (2000).

[6] Sol, A., and Van-Herpe, F."Numerical prediction of a whole car vibroacoustic behavior at low frequencies," *SAE 2001 Noise and Vibration Conference proceedings* CDROM ISBN 0-7680-0775-5 (2001)

[7] Soize, C. "Random matrix theory for modeling random uncertainties in computational mechanics," *Comp. Meth. Appl. Mech. Eng.* 194(12-16), 1333-1366. (2005)

[8] Soize, C."A comprehensive overview of a non-parametric probablistic approach of model uncertainties for predictive models in structural dynamics," *J. Sound Vib.* 288(3), 623-652 (2005)

[9] Serfling, R .J. "Approximation Theorems of Mathematical Statistics", John Wiley & Sons. (1980)

[10] Spall, J.C. "Introduction to Stochastic Search and Optimization", John Wiley and Sons, Hoboken, New Jersey. (2003)

[11] Walter, E., and Pronzato, L. "Identification of Parametric Models from Experimental Data", Springer (1997)